**PIER M**

# Triband Dual Port H-SRR MIMO Antenna for WLAN/WiMAX/Wi-Fi 6 Applications

Puneet Sehgal[1, 2] and Kamlesh Patel[2, *]

[1]*Atma Ram Sanatan Dharma College, University of Delhi, Dhaula Kuan, New Delhi 110021, India*
[2]*Department of Electronic Science, University of Delhi South Campus, New Delhi 110021, India*

**ABSTRACT:** A CPW-fed hexagon-shaped split ring resonator (H-SRR) antenna consisting of three concentric SRR rings is proposed for triband WLAN/WiMAX and Wi-Fi6 applications. A single port optimized antenna has a size of $43 \times 22 \times 1.6 \, \text{mm}^3$ with two ports, and a multiple-in-multiple-out (MIMO) antenna based on the same H-SRR design is of size $95 \times 52 \times 1.6 \, \text{mm}^3$. The use of metallic loadings between the rings led to an impedance bandwidth of 21%/65% for the single-port H-SRR antenna and 33%/66.5% for the dual-port H-SRR antenna in the 2.4 GHz band and 5.2/6 GHz bands. The antennas exhibit a gain in the range of 2–2.7 dB and good radiation characteristics. Also, the proposed antenna design achieves the isolation of more than 30 dB without using any de-coupling network making the structure simple and compact. For tri-band applications of the proposed dual port antenna, the MIMO parameters ECC, TARC, DG, and MEG are found about $< 0.005$, $< -10 \, \text{dB}$, $\leq 10 \, \text{dB}$, and $< -6 \, \text{dB}$, respectively in the 2.4/5.2/6 GHz bands without any decoupling structure. Measurements with a commercial transmitter at 5.8 GHz confirmed that these antennas offer better Wi-Fi 6 connectivity. Thus, the results confirm that the novel features of the proposed antennas are simple structure, wideband operation, and moderate gain with a compact size in the 2.4/5.2/6 GHz bands, and therefore, these presented antennas are useful in the current WLAN/WiMAX systems as well as upcoming Wi-Fi 6 applications like routers.

## 1. INTRODUCTION

In this digital world, Wireless Fidelity (*Wi-Fi*) as a form of internet network is enabling superfast, reliable access via connecting several devices wirelessly, like computers, smartphones, televisions, video game consoles, etc. Many WiFi Service Management Platforms have been developed including Authentication, Billing, Location-aware Services, Captive Portal, Subscriber Analytics, Mobile App, etc. So, it is currently very difficult to have a good means of communication with better internet connectivity without a greater rate of data transmission, which is in enormous demand in many places, such as in congested areas, in a family where many users are present, offices, universities, colleges, and malls [1]. Also, there is a critical need to increase a network's capability. Typically, the Wi-Fi frequencies are 2.4 GHz and 5 GHz, which is now extended up to 6 GHz by the new next-generation Wi-Fi standard known as Wi-Fi 6 (802.11 ax) for better and faster connectivity. This Wi-Fi 6 is devised as the latest technology to resolve the above issues [2]. This technology of Wi-Fi 6 has become quite popular as it is capable of providing the maximum data rate of up to 9.6 Gb/s while maintaining strong connections even when more and more devices are added [3]. Further, this technology of Wi-Fi 6 has many advantages like reliability, efficiency, flexibility, security, and scalability of the network [4] for better working of the complex network with a high density of interconnected systems working parallelly. To cover Wi-Fi6 along with the existing WLAN/WiMAX technologies, various multiband or wideband antennas have

been reported which utilized complementary spilt ring resonator (CSRR) [5], printed graphite paper [6], slots [7], I-shaped slots and shorted vias [8], shark-fin [9], frequency reconfigurable [10], and multiple resonator stubs [11] for wireless applications. Also, complex structure coplanar waveguide (CPW)-fed metamaterial-inspired antennas were presented using Composite Right/Left Handed (CRLH) metamaterial for Bluetooth and WLAN/Wi-Fi applications [12, 13], whereas a modified split-ring resonator-based short-ended metamaterial antenna was discussed, which covered only Wi-Max applications [14]. A coplanar waveguide-fed planar antenna was proposed only to cover IEEE 802.11ac applications with reduced radiation hazards [15, 16]. So, the widespread use of the newest technologies, like Wi-Fi 6 and many others, makes it easiest to understand how the utility of technology improves among the general public as it develops. Monopole or CPW-fed antennas face certain problems like bandwidth and size limitation, moderate radiation pattern, etc. to utilize in Wi-Fi 6 applications. To overcome such issues, multiple-input multiple-output (MIMO) antenna is proposed in past to remove the problem of interfacing between various devices and to improve connectivity between the systems thus increasing the system reliability for better future aspects. In addition, MIMO antenna offers higher data rates, improved reliability, and increased capacity with better coverage which make it a desirable choice for Wi-Fi 6 applications over a traditional single antenna [17–19].

Recently, a few wideband MIMO antennas have been reported for Wi-Fi 5 and Wi-Fi 6 applications with good isolation [1, 17–19], and various multiband antennas have been reported with different structures, like flexible antenna formed by

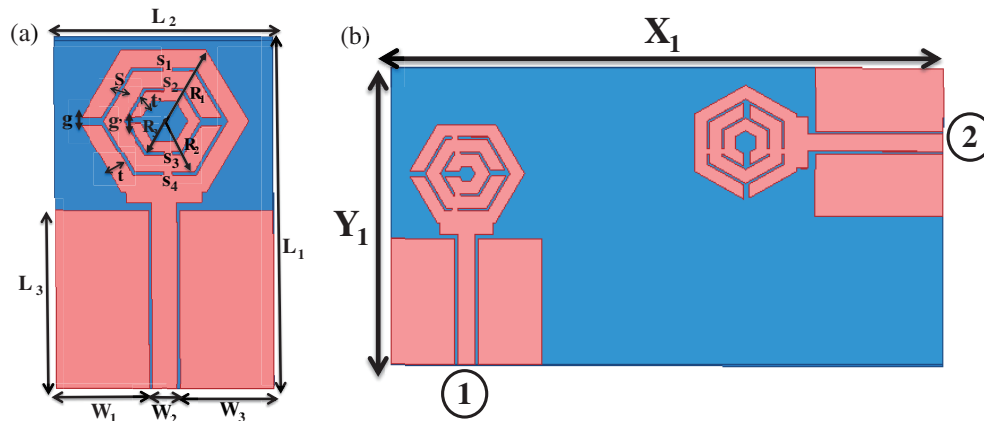* Corresponding author: Kamlesh Patel (kpatel@south.du.ac.in).

**FIGURE 1**. Schematics of (a) proposed single port H-SRR triband antenna design, and (b) proposed dual port H-SRR triband antenna design.

an inverted E and inverted L-shaped conductive structure and a truncated ground with a vertical stub [20], low-SAR penta-band microstrip patch antenna [21], compact tri-band antenna with double winding structures [22], microstrip patch antenna based on modified SRR and modified CSRR as defected ground plane [23], etc. Still, these antennas had many issues like large sizes, complex structural designs, limited bandwidth, and nonuniform antenna performance over triband frequencies, i.e., 2.4/5.2/6 GHz. To overcome these issues, this paper presents a simple, compact, cost-effective, easy-to-manufacture CPW-fed hexagon-shaped split ring resonator (H-SRR) antenna with a single port and dual port excitations with a simple structure for WLAN/ WiMax and Wi-Fi 6 applications. The proposed antennas are built on a low-cost FR-4 substrate, and the main radiator is composed of a hexagon-shaped resonator ring structure with three concentric rings fed with a CPW structure. The return loss, $S$-parameters, gain, and radiation pattern are discussed for the triband frequency of 2.4/5.2/6 GHz. Further, the MIMO parameters of the dual-port antenna are evaluated, and its parameters are found in the desired range without using any decoupling structure for Wi-Fi 6 bands.

## 2. DESIGN AND ANALYSIS OF HEXAGONAL SRR TRIBAND ANTENNA

The single port hexagonal split ring resonator (H-SRR) antenna of variable thickness of the rings is designed on ANSYS HFSS software by taking an FR-4 substrate with parameters $\varepsilon_r = 4.4$, $h$ (height of the substrate) = 1.5 mm, loss tangent = 0.02 and 35 µm thick copper layer. The single H-SRR antenna is optimized to get a response at the desired frequencies in the 2.4/5.2/6.0 GHz range for WLAN and Wi-Fi 6 applications. As shown in Figure 1(a), the single port H-SRR antenna is fed with CPW and consists of three split-ring resonator rings of hexagonal shape with outer radius ($R_1$), a middle ring with radius ($R_2$) and inner radius ($R_3$), respectively. The optimized dimensions are given in Table 1. The proposed single port H-SRR triband antenna design is of size $43 \times 26 \times 1.6$ mm$^3$ while the dual port antenna is of size $95 \times 52 \times 1.6$ mm$^3$. Figure 1(b) shows the proposed dual port H-SRR antenna design with CPW feed, which

is optimized to get higher gain values with sufficient isolation at the 2.4/5.2/6.0 GHz bands than the single port antenna.

### 2.1. Return Loss, Various S-Parameters of the Proposed Single Port and Dual Port Triband H-SRR Antenna

Figure 2(a) shows the measurement setup using R&S VNA model ZVH8 to measure the return loss ($S_{11}$) of the antenna after calibration. The simulated and measured return losses (RLs) of single port and dual port triband H-SRR antennas are shown in Figures 2(b) and (c), respectively. It can be observed in Figure 2(b) that the simulated RL for the single port antenna is $-20.27/-11.25/-18.67$ dB at 2.4/5.2/6 GHz while measured values are $-15.45/-12.90/-13.70$ dB. Although the dual port H-SRR antenna shows improved values of simulated return loss $-21.61/-17.67/-20.59$ dB, the measured values of $-21.01/-14.91/-13.13$ dB are in the acceptable range at 2.4/5.2/6 GHz frequency bands, respectively, due to fabrication tolerances.

The simulated impedance bandwidths (IBWs) for the single port antenna and dual port antenna are found 20/70.39/61% and 30/71.54/62% at the 2.4/5.2/6.0 GHz bands, respectively. In Figure 2(c), the simulated scattering ($S$) parameters $S_{12}/S_{21}$ of the dual-port triband antenna are obtained as $-22.59/-35.42/-31.69$ dB, whereas the measured $S_{12}/S_{21}$ are $-22.85/-31.14/-28.98$ dB at 2.4/5.2/6 GHz which confirms the sufficient isolation between ports 1 and 2 without any decoupling structure required. The simulated and measured $S_{22}$ of dual port H-SRR antenna are found to be $-15.28/-17.29/-15.91$ dB and $-14.66/-19.02/-13.75$ dB, respectively at frequency bands of 2.4/5.2/6 GHz, which signifies that the antenna is efficiently radiating the signal from either port without reflecting towards the other port.

### 2.2. Gain and Radiation Pattern Performance Proposed Single Port and Dual Port Triband H-SRR Antenna

For the gain response in Figure 3(a), the maximum simulated gain of 2.7 dB is obtained at 6.32 GHz for single port H-SRR antenna whereas 2.56/3.20 dB is obtained for dual-port antenna at 5.27/6.56 GHz on exciting port 1 and port 2, respectively, while another port is matched.

**TABLE 1**. Optimized dimensions of proposed triband H-SRR antenna designs.

| Various dimensions | Values (in mm) |
|---|---|
| Length of the ground planes ($L_1$) | 43 |
| Length of the patch ($L_2$) | 22 |
| Widths of top grounds ($W_1 = W_3$) | 11 |
| Width of the center CPW line ($W_2$) | 3 |
| Metallic loadings ($S_1 = S_2 = S_3 = S_4$) | $1 \times 1\,\mathrm{mm}^2$ |
| Gap within outermost and middle rings ($g$) | 1 |
| Gap within innermost rings ($g'$) | 0.75 |
| Spacing between the rings ($S$) | 0.5 |
| Thickness of outermost and middle rings ($t$) | 2.5 |
| Thickness of innermost rings ($t'$) | 1.5 |
| Radius of the outermost ring ($R_1$) | 10 |
| Radius ($R_2$) | 7 |
| Radius of innermost ring ($R_3$) | 4 |
| $X_1$ | 95 |
| $Y_1$ | 52 |
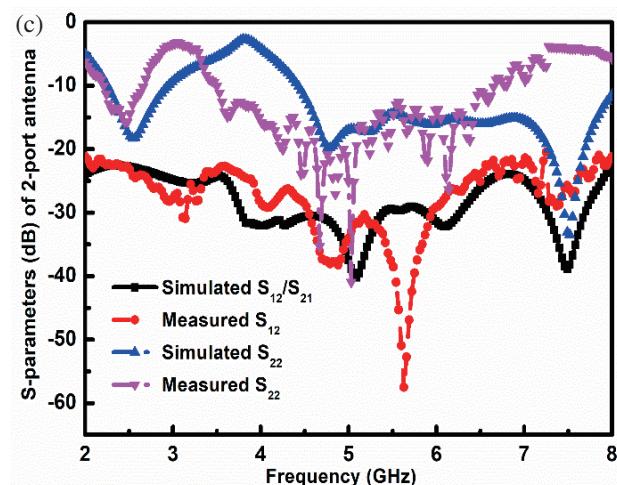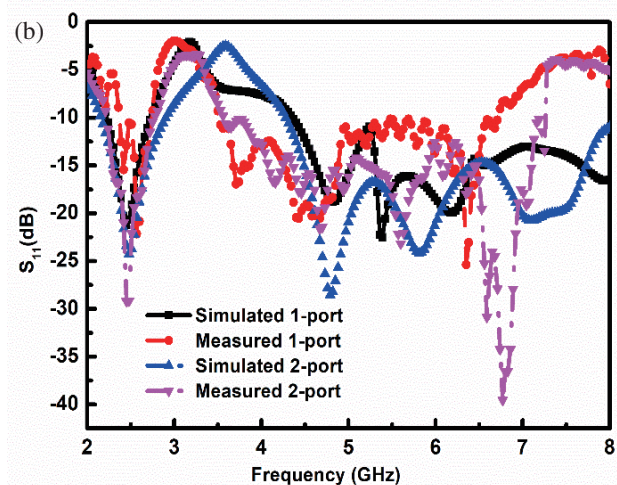


**FIGURE 2**. (a) Measurement setup with R&S VNA ZVH8 in the anechoic chamber. (b) Simulated and measured return loss ($S_{11}$) performance of single port and dual port triband HSRR antenna, and (c) Simulated and measured $S_{12}/S_{21}$, $S_{22}$ parameters of dual port triband HSRR antenna.
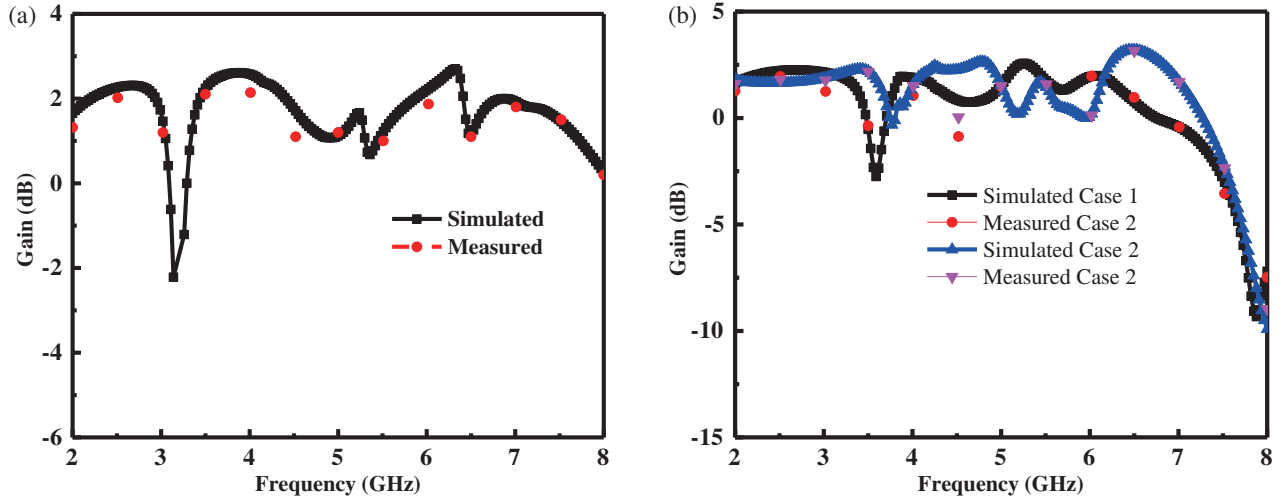
**FIGURE 3**. Gain characteristics of (a) single port H-SRR triband antenna and (b) dual port for case 1 and case 2.

At 2.4/5.2/6.0 GHz, the single port antenna is reported to have the simulated gain of 2.2/1.63/2.23 dB compared to the measured gain of 2.02/1.0/1.87 dB as in Figure 3(a). In Figure 3(b), the simulated gain values obtained for dual port H-SRR antenna are 2.18/2.53/1.96 dB for case 1 (when port 1 is excited and port 2 matched), and the measured values obtained are 1.94/1.53/1.97 dB while in case 2 (when port 2 is excited and port 1 matched), the antenna provides the simulated gain of 1.65/0.2/0.198 dB and measured gain of 1.8/1.59/0.12 dB at 2.4/5.2/6.0 GHz frequencies, respectively. Significant and moderate gain values are observed for simultaneous transmission/receptions in these bands by the proposed antennas.

Figures 4(a)–(f) show the simulated and measured 2-D radiation patterns of the proposed dual port triband H-SRR antenna for $E$-plane ($X$-$Z$) and $H$-plane ($X$-$Y$), respectively. As the omnidirectional pattern results in $H$-plane, and a dumbbell-shaped pattern is obtained for the $E$-plane at 2.4/5.2/6.0 GHz frequency bands, this triband H-SRR antenna is promising for WLAN/WiMAX and Wi-fi 6 applications.

The simulated surface current distributions of dual port H-SRR antenna are shown in Figures 5(a)–(c) at resonant frequencies, 2.4 GHz, 5.2 GHz, and 6.0 GHz, respectively. At 2.4 and 5.2 GHz, the maximum radiation is contributed by the first and second rings of the SRR structure and the central conductor of the CPW feed, whereas the maximum radiation is contributed by the innermost ring along with the central CPW feed line structure at 6.0 GHz.

## 3. DIVERSITY CHARACTERISTICS OF THE PROPOSED DUAL PORT H-SRR TRIBAND ANTENNA

Further, the diversity performance of the proposed dual port H-SRR triband antenna is studied by evaluating the envelope correlation coefficient (ECC), total active reflection coefficient (TARC), diversity gain (DG), and mean effective gain (MEG). For the proposed antenna, the ECC between two antenna elements, i.e., antenna $k$ and antenna $l$, can be obtained from their far-field radiation patterns using Equation (1) [24].

$$\text{ECC} = \frac{\left| \iint_{4\pi} \bar{F}_k\left(\theta,\psi\right) \cdot \bar{F}_l^*\left(\theta,\psi\right) d\Omega \right|^2}{\iint_{4\pi} \left| \bar{F}_k\left(\theta,\psi\right) \right|^2 d\Omega \iint_{4\pi} \left| \bar{F}_l\left(\theta,\psi\right) \right|^2 d\Omega} \quad (1)$$

where the complex vectors, $\bar{F}_k\left(\theta,\psi\right)$ and $\bar{F}_l\left(\theta,\psi\right)$, are the far-field radiation patterns of antenna $k$ and antenna $l$, respectively, and * represents the Hermitian transpose of the matrix [25]. The ECC can also be obtained by using the $S$-parameters of the antenna [24] as

$$\text{ECC} = \frac{\left| S_{kk}^* S_{kl} + S_{lk}^* S_{ll} \right|^2}{\left( 1 - \left| S_{kk} \right|^2 - \left| S_{kl} \right|^2 \right)\left( 1 - \left| S_{lk} \right|^2 - \left| S_{ll} \right|^2 \right)} \quad (2)$$

TARC is defined as the ratio of root square total reflected power ($a_i$) to root square total incident power ($b_i$) by the antenna, and for the M-port antenna, it is obtained from Equation (3) in terms of $S$-parameters for two ports [24].

$$\text{TARC} = \sqrt{\frac{(S_{11}+S_{12}e^{j\varphi})^2+(S_{21}+S_{22}e^{j\varphi})^2}{2}} \quad (3)$$

where $\varphi$ is the phase of the associated S-parameter.

Next, the diversity gain (DG) is obtained using Equation (4), which is defined as the amount of transmitted power that can be reduced without any loss in the diversity technique [24, 25].

$$\text{DG} = 10\sqrt{1 - (\text{ECC}^2)} \quad (4)$$

MEG represents the ratio of average received power by a diversity antenna at a single port to the power received by an isotropic antenna in the operating band. It is desirable to be between $-3$ dB and $-12$ dB to ensure an equal power ratio to each antenna element [25]. For the M-port antenna system, MEG can be evaluated from $S$-parameters ($S_{kC}$) as follows [25]

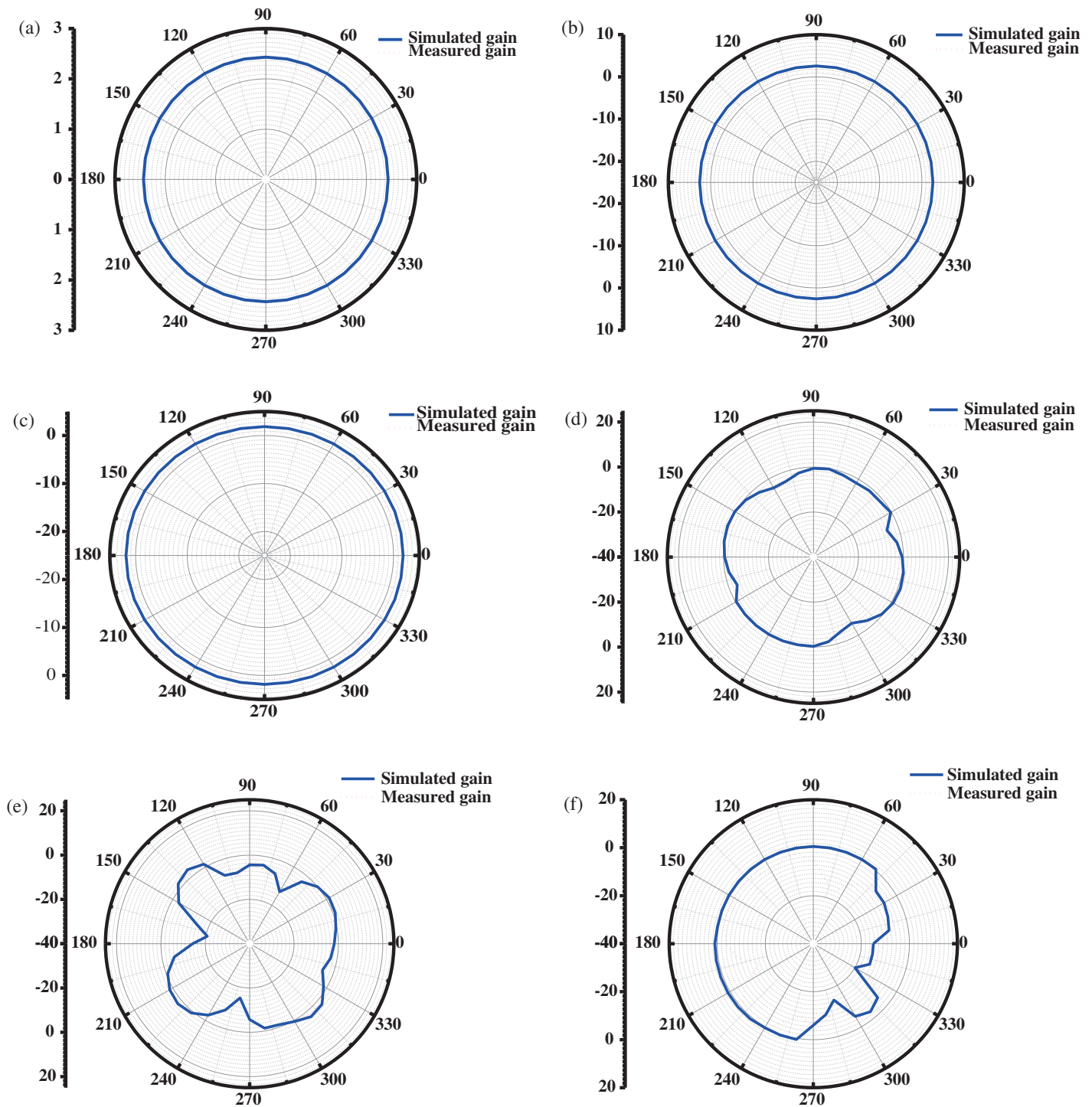$$\text{MEG}_k = 0.5 \left( 1 - \sum_{C=1}^{M} \left| S_{kC} \right|^2 \right) \quad (5)$$

**FIGURE 4**. 2-D radiation patterns of dual port H-SRR antenna for case 1 (a) $H$-plane at 2.4 GHz, (b) $H$-plane at 5.2 GHz, (c) $H$-plane at 6.0 GHz, (d) $E$-plane at 2.4 GHz, (e) $E$-plane at 5.2 GHz, and (f) $E$-plane at 6.0 GHz.

where $M$ is the number of antennas, and $k$ $(= 1,\ 2)$ is the active antenna.

The measured MIMO parameters are obtained from the measured $S$-parameters of the proposed MIMO antenna [24]. Figure 6(a) shows that simulated and measured ECCs are found to be less than 0.005 in the frequency band of 2.4/5.2/6.0 GHz range for the dual port H-SRR triband antenna, and con-

firms the efficient working of the proposed MIMO antenna for WLAN/WiMAX/Wi-Fi-6 systems. Figure 6(b) shows that the simulated and measured TARC values are less than $-10$ dB at most frequencies in 2.4/5.2/6.0 GHz bands, while the MIMO antenna exhibits DG about 10 dB in the complete band except a notch near 3.6 GHz, and so acceptable for WLAN/WiMAX and Wi-Fi 6 applications. The simulated and measured MEG val-
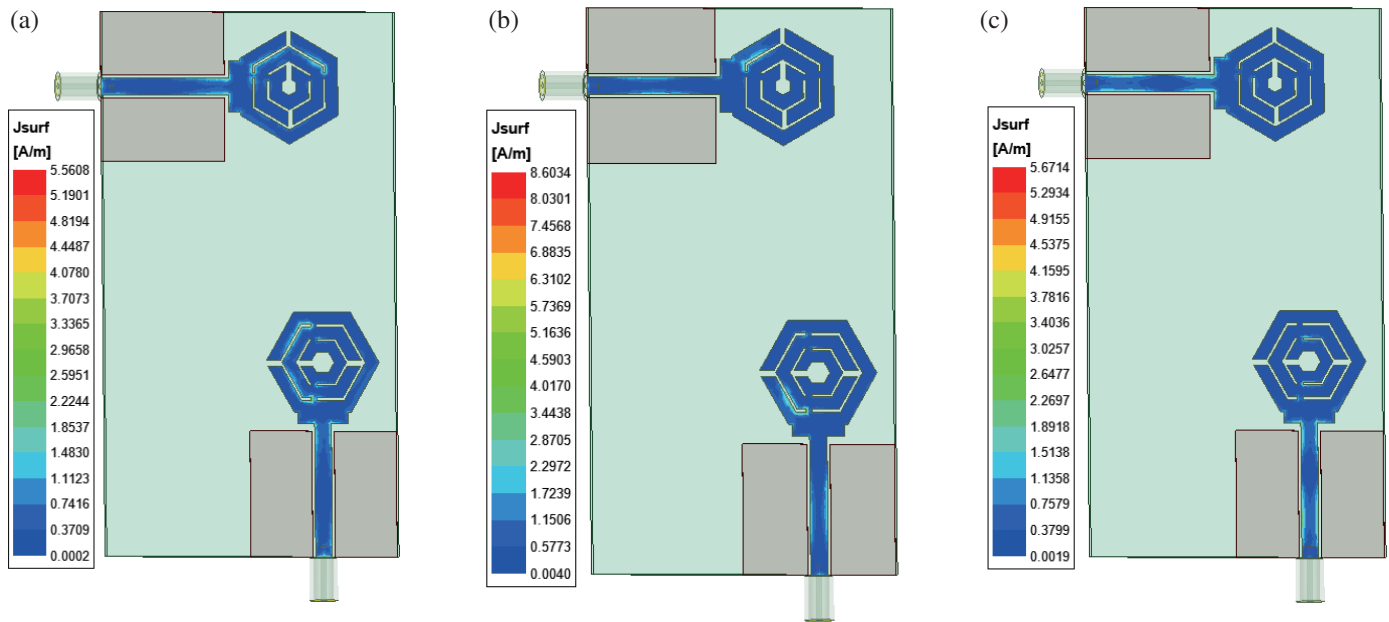
**FIGURE 5**. The surface current distribution of dual-port H-SRR antenna at (a) 2.4 GHz, (b) 5.2 GHz, and (c) 6 GHz.
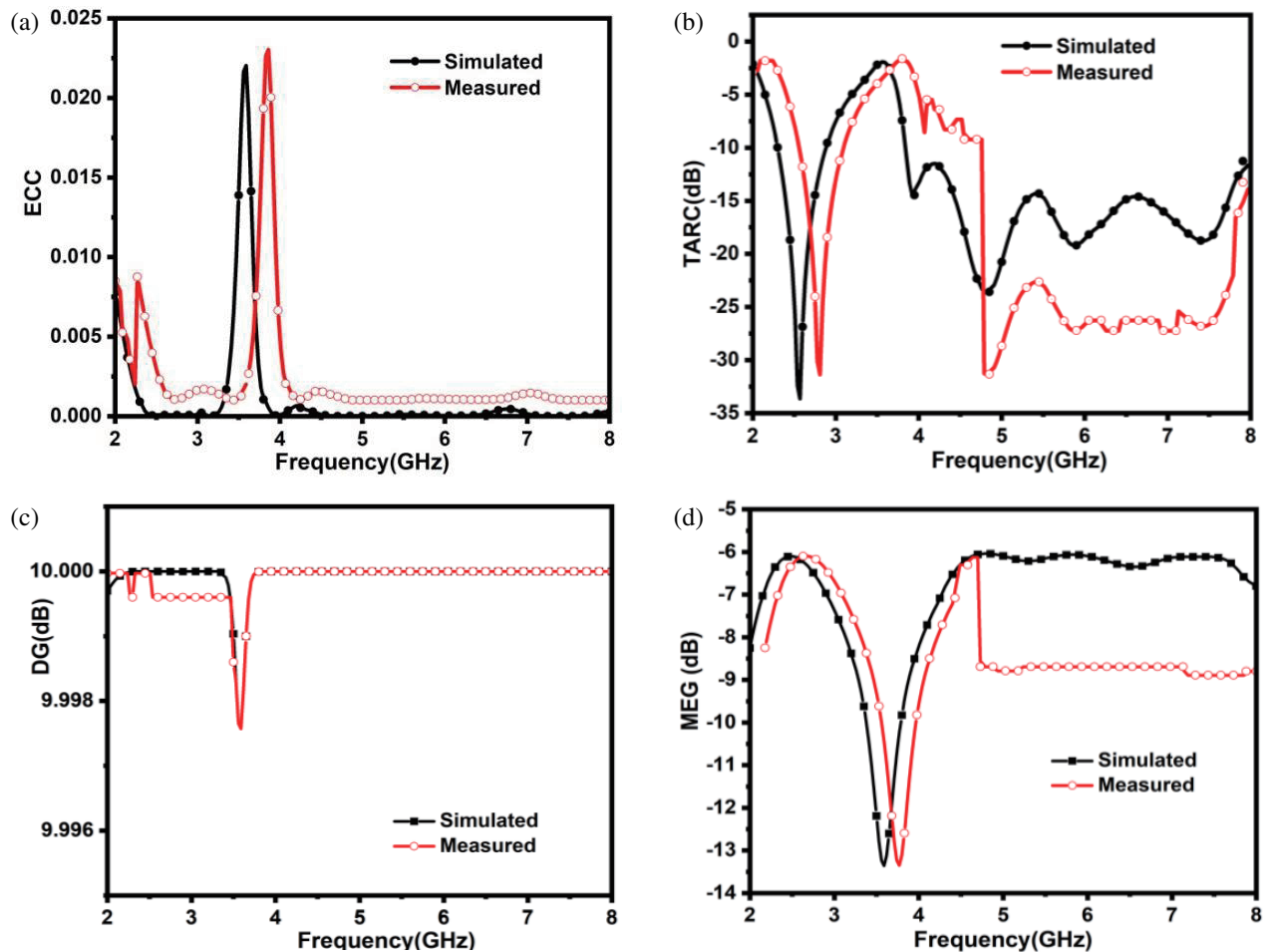


**FIGURE 6**. MIMO performance of dual port H-SRR antenna, (a) ECC, (b) TARC, (c) DG, and (d) MEG.
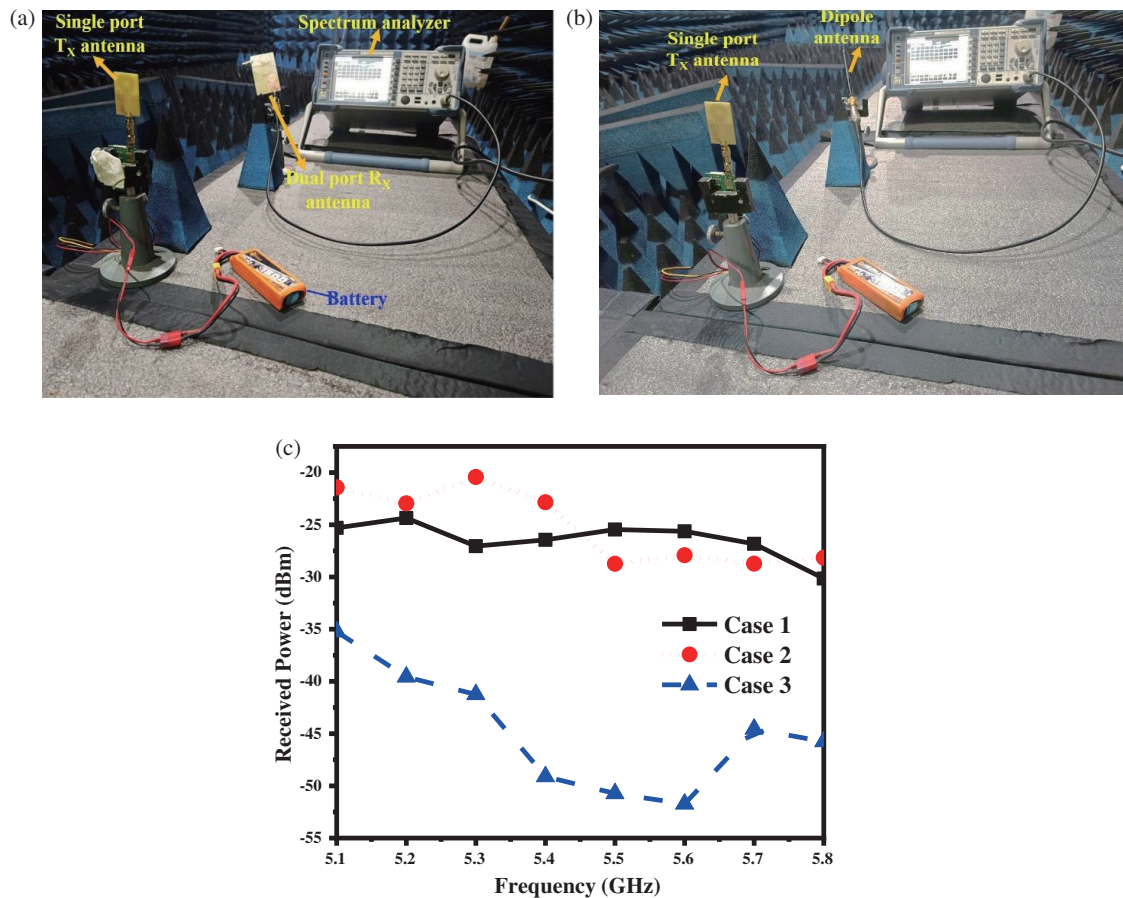
FIGURE 7. Measurement set up (a) for case 1, (b) case 3, (c) responses of received powers in the Wi-Fi-6 band.

ues of the proposed antenna are found to be $-6.13/-6.12/-6.10$ dB and $-6.69/-8.69/-8.73$ dB in the 2.4/5.2/6.0 GHz bands, respectively. The measured results are slightly shifted towards high frequency due to being governed by measured $S$-parameters shown in Figs. 2(b)–(c), however, fulfilling the desired MIMO performance.

A comparison with the previously published antennas is shown in Table 2 to show the novelty of the proposed H-SRR antenna design.

Based on Table 2, the salient and important features of the proposed H-SRR antenna designs are as follows:

1. The proposed antenna is compact with smaller dimensions than the antennas in [9–11] and less in thickness than the antennas in [2, 8–14].

2. The proposed antenna has a higher gain than the antennas in [4–6, 9].

3. The proposed antenna is cost-effective as it does not use an expensive RT-Duroid substrate unlike [6, 8] with lower fabrication cost.

4. The proposed antenna has a simple design structure, comparatively [20–23].

5. The proposed MIMO antenna attained an isolation of more than 22 dB without any decoupling structure.

Thus, the proposed triband dual port MIMO antenna with these features can overcome the effect of spurious radiation

without much power loss and is also able to provide wide bandwidth operation in the triband frequencies as compared to most of the previous designs, so it is a suitable candidate for WLAN/WiMAX and Wi-Fi 6 applications. To show the impact of proposed triband H-SRR antennas, the Wi-Fi 6 connectivity is studied using the setup in the anechoic chamber shown in Figs. 7(a), (b), in which the single port triband H-SRR antenna is connected as a transmitting antenna ($T_X$) to the TS832 5.8 GHz AV transmitter operated by an 11.1 V battery.

On the other hand, the dual port triband MIMO H-SRR antenna is connected as a receiver antenna ($R_X$) which is connected to spectrum analyzer (SA) model R&S FSL6 to measure the power received. The separation between the two antennas is kept around 35 cm ($d$). The following three cases are considered to analyze for better Wi-Fi-6 connectivity:

Case 1: When Port 1 of the $R_X$ MIMO antenna is connected to SA, and its Port 2 is with a 50 Ω termination.

Case 2: When Port 2 of the $R_X$ MIMO antenna is connected to SA, and its Port 1 is with a 50 Ω termination.

Case 3: When a standard dipole antenna of 5.8 GHz is used as an $R_X$ antenna and connected to SA.

The received power is measured for the above three cases in the frequency band from 5.1 to 5.8 GHz obtained by varying the TS832 transmitter channels, which generate signals with a power of 600 mW. Fig. 7(c) shows that the received power is

**TABLE 2**. Comparison between the present work and previously works.

| Refs. | Shape of antenna | $\varepsilon_r$ of the substrate | Frequency (GHz) | Size (mm³) | Gain (dB) | Feeding technique |
|---|---|---|---|---|---|---|
| [1] | Oval shaped | FR-4 | 5/6 | $20 \times 8.7 \times 0.4$ | 2.25 | CPW |
| [2] | Hexagonal shaped | FR-4 | 0.9/2.4/5.2 | $18 \times 22 \times 1.6$ | – | CPW |
| [7] | Rectangular and circular slots | FR-4 | 2.4/3.3/5.8 | $17.5 \times 8 \times 0.8$ | 1.5 | Microstrip |
| [9] | shark-fin shaped | FR-4 | 0.8/1.7/2.4/5 | $57 \times 40 \times 1.6$ | 6.7 | Co-axial |
| [10] | Hexagonal shaped | FR-4 | 3.3/5/6.6/9.9 | $44 \times 39 \times 1.6$ | 1.98 | Microstrip |
| [11] | Multiple resonant stubs | FR-4 | 2.4/3.8/5 | $43 \times 33 \times 1.6$ | 5.6 | Microstrip |
| [14] | Circular SRR shaped | FR-4 | 3.17/5.39 | $20 \times 25.5 \times 1.6$ | 0.71, 1.89 | CPW |
| [20] | E and L-shaped | FR-4 | Sub-6 GHz 5G and X-band | $987 \ (0.612\lambda^2)$ | – | CPW |
| [21] | Rectangular | FR-4 | (2.95–3.06), (3.79–3.87), (4.11–4.19), (5.39–5.51), and (5.97–6.11) | $26 \times 30 \times 1.6$ | 6.2 | CPW |
| [22] | Double winding structure | FR-4 | 2.9/6.5/11.3 | $18.6 \times 15.6 \times 1.6$ | 1.9, 5.2 | CPW |
| [23] | Rectangular shaped | FR-4 | 2.8/5.8/6.9 | $35 \times 35 \times 1.6$ | 3.62, 3.48, 3.22 | CPW |
| **This work** | **Single port H-SRR triband** | **FR-4** | **2.4/5.2/6.0** | $43 \times 26 \times 1.6$ | **2.31/1.6/2.7** | **CPW** |
|  | **Dual port H-SRR triband** | **FR-4** | **2.4/5.2/6.0** | $95 \times 52 \times 1.6$ | **2.26/2.53/1.99** | **CPW** |

in the range of $-20$ to $-26$ dBm for Case 1 and Case 2 of the dual port MIMO antenna without changing its angular position, while it is $-35$ to $-53$ dBm when the dipole antenna is used as $R_X$ antenna in Wi-Fi 6 band. Thus, the proposed MIMO H-SRR antenna is a potential candidate to achieve better Wi-Fi-6 connectivity, and the vector addition of the signals from both the ports ensures a strong and reliable reception.

## 4. CONCLUSION

A novel, cost-effective simple triband single port and dual port H-SRR antennas are studied successfully. The dual port H-SRR triband proposed antenna has a low profile of $95 \times 52 \times 1.6$ mm³ on an FR-4 substrate and achieves the improved impedance

bandwidth along with a moderate gain at triband frequencies of 2.4/5.2/6.0 GHz. Both H-SRR antennas are fabricated, and their measured return loss values, $S$-parameters, gain values, and 2-D radiation patterns are found in good agreement with the simulated ones. The simulated and measured MIMO parameters, ECC, TARC, DG, and MEG are obtained to verify the diversity performance of dual port H-SRR triband antenna and are found to be within the desired values. Compared to the standard dipole, these antennas are effective for Wi-Fi 6 connectivity due to higher gain and better impedance bandwidth. Therefore, these triband antennas can be suitable for the use in WLAN/WiMAX and Wi-Fi 6 communications according to IEEE 802.11ax standards in next-generation wireless devices.

**PIER M**

## REFERENCES

[1] Kulkarni, J. and C.-Y.-D. Sim, "Wideband CPW-fed oval-shaped monopole antenna for Wi-Fi5 and Wi-Fi6 applications," *Progress In Electromagnetics Research C*, Vol. 107, 173–182, 2021.

[2] Rajalakshmi, P. and N. Gunavathi, "Compact modified hexagonal spiral resonator based tri-band patch antenna with octagonal slot for Wi-Fi/WLAN applications," *Progress In Electromagnetics Research C*, Vol. 106, 77–87, 2020.

[3] Kulkarni, J. S., "An ultra-thin, dual band, sub 6 GHz, 5G and WLAN antenna for next generation laptop computers," *Circuit World*, Vol. 46, No. 4, 363–370, Oct. 2020.

[4] Rajalakshmi, P. and N. Gunavathi, "Hexagonal split ring resonator enclosed circular split ring resonator inspired dual-band antenna for sub-6 GHz 5G NR and IEEE 802.11 ba/be applications," *Progress In Electromagnetics Research C*, Vol. 115, 1–15, 2021.

[5] Kumar, N. R., P. D. Sathya, S. K. A. Rahim, M. Z. M. Nor, A. Alomainy, and A. A. Eteng, "Compact tri-band microstrip patch antenna using complementary split ring resonator structure," *Applied Computational Electromagnetics Society Journal*, Vol. 36, No. 3, 346–353, Mar. 2021.

[6] Aziz, A. A. A., A. T. Abdel-Motagaly, A. A. Ibrahim, W. M. A. E. Rouby, and M. A. Abdalla, "A printed expanded graphite paper based dual band antenna for conformal wireless applications," *Aeu-international Journal of Electronics and Communications*, Vol. 110, 152869, 2019.

[7] Kulkarni, J. and C.-Y.-D. Sim, "Low-profile, compact multiband monopole antenna for futuristic wireless applications," in *2020 IEEE International Conference on Electronics, Computing and Communication Technologies (CONECCT)*, 1–5, 2020.

[8] Kumar, A., A. A. Althuwayb, and M. J. Al-Hasan, "Wideband triple resonance patch antenna for 5G Wi-Fi spectrum," *Progress In Electromagnetics Research Letters*, Vol. 93, 89–97, 2020.

[9] Abbasi, N. A., R. Langley, and S. Bashir, "Multiband shorted monopole antenna," *Journal of Electromagnetic Waves and Applications*, Vol. 28, No. 5, 618–633, Mar. 2014.

[10] Saraswat, R. K. and M. Kumar, "A vertex-fed hexa-band frequency reconfigurable antenna for wireless applications," *International Journal of RF and Microwave Computer-aided Engineering*, Vol. 29, No. 10, Oct. 2019.

[11] Jing, J., J. Pang, H. Lin, Z. Qiu, and C.-J. Liu, "A multiband compact low-profile planar antenna based on multiple resonant stubs," *Progress In Electromagnetics Research Letters*, Vol. 94, 1–7, 2020.

[12] Rajalakshmi, P. and N. Gunavathi, "Compact modified hexagonal spiral resonator based tri-band patch antenna with octagonal slot for Wi-Fi/WLAN applications," *Progress In Electromagnet-*

*ics Research C*, Vol. 106, 77–87, 2020.

[13] Gupta, A. and R. K. Chaudhary, "A compact dual band short ended metamaterial antenna with extended bandwidth," *International Journal of RF and Microwave Computer-aided Engineering*, Vol. 26, No. 5, 435–441, Jun. 2016.

[14] Kukreja, J., D. K. Choudhary, and R. K. Chaudhary, "CPW fed miniaturized dual-band short-ended metamaterial antenna using modified split-ring resonator for wireless application," *International Journal of RF and Microwave Computer-aided Engineering*, Vol. 27, No. 8, Oct. 2017.

[15] Gunavathi, N. and D. Sriramkumar, "CPW-fed monopole antenna with reduced radiation hazards toward human head using metallic thin-wire mesh for 802.11ac applications," *Microwave and Optical Technology Letters*, Vol. 57, No. 11, 2684–2687, 2015.

[16] Gunavathi, N. and D. S. Kumar, "Miniaturized unilateral coplanar waveguide-fed asymmetric planar antenna with reduced radiation hazards for 802.11ac applications," *Microwave and Optical Technology Letters*, Vol. 58, No. 2, 467–471, Feb. 2016.

[17] Zhang, W., Y. Li, K. Wei, and Z. Zhang, "A two-port microstrip antenna with high isolation for Wi-Fi 6 and Wi-Fi 6e applications," *IEEE Transactions on Antennas and Propagation*, Vol. 70, No. 7, 5227–5234, Jul. 2022.

[18] Sim, C.-Y.-D., H.-Y. Liu, and C.-J. Huang, "Wideband MIMO antenna array design for future mobile devices operating in the 5G NR frequency bands n77/n78/n79 and LTE band 46," *IEEE Antennas and Wireless Propagation Letters*, Vol. 19, No. 1, 74–78, Jan. 2020.

[19] Kulkarni, J., A. Desai, and C.-Y. D. Sim, "Wideband four-port MIMO antenna array with high isolation for future wireless systems," *AEU-International Journal of Electronics and Communications*, Vol. 128, 153507, Jan. 2021.

[20] Kulkarni, N. P., N. B. Bahadure, P. D. Patil, and J. S. Kulkarni, "Flexible interconnected 4-port MIMO antenna for sub-6 GHz 5G and X band applications," *AEU-International Journal of Electronics and Communications*, Vol. 152, Jul. 2022.

[21] Manikandan, M. and S. K. Lakshmi, "A compact penta-band low-SAR antenna loaded with split-ring resonator for mobile applications," *International Journal of Antennas and Propagation*, Vol. 2022, Dec. 2022.

[22] Prasanna, R., P. Saravanan, and S. Rajarajan, "Compact tri-band antenna with double winding structures for 3G/4G/5G base station applications," *Wireless Personal Communications*, Vol. 129, No. 1, 371–386, Mar. 2023.

[23] Joe, D. A. and T. Krishnan, "A triband compact antenna for wireless applications," *International Journal of Antennas and Propagation*, Vol. 2023, Sep. 2023.

[24] Kaushal, V., A. Birwal, and K. Patel, "Diversity characteristics of four-element ring slot-based mimo antenna for sub-6-GHz applications," *ETRI Journal*, Vol. 45, No. 4, 581–593, Aug. 2023.

[25] Pahadsingh, S. and S. Sahu, "Four port MIMO integrated antenna system with DRA for cognitive radio platforms," *AEU-International Journal of Electronics and Communications*, Vol. 92, 98–110, 2018.